


RESEARCH ARTICLE OPEN ACCESS

Phase Locking of 40 Hz Auditory Steady State Responses Is Modulated by Sensory Predictability and Linked to Cerebellar Myelination

Kit Melissa Larsen^{1,2} | Kiran Thapaliya³ | Markus Barth^{4,5} | Chin-Husan Sophie Lin⁶  | Hartwig R. Siebner^{1,7,8} | Marta I. Garrido^{2,6,9}

¹Danish Research Centre for Magnetic Resonance, Department of Radiology and Nuclear Medicine, Copenhagen University Hospital - Amager and Hvidovre, Copenhagen, Denmark | ²Queensland Brain Institute, The University of Queensland, Saint Lucia, Australia | ³National Centre for Neuroimmunology and Emerging Diseases, Griffith University, Nathan, Australia | ⁴Centre for Advanced Imaging, The University of Queensland, Brisbane, Queensland, Australia | ⁵School of Information Technology and Electrical Engineering, The University of Queensland, Brisbane, Queensland, Australia | ⁶Melbourne School of Psychological Sciences, The University of Melbourne, Melbourne, Australia | ⁷Department of Clinical Medicine, Faculty of Health and Medical Sciences, University of Copenhagen, Copenhagen, Denmark | ⁸Department of Neurology, Copenhagen University Hospital Bispebjerg, Copenhagen, Denmark | ⁹Graeme Clark Institute for Biomedical Engineering, The University of Melbourne, Melbourne, Australia

Correspondence: Kit Melissa Larsen (melissal@drcmr.dk)

Received: 28 October 2024 | **Revised:** 22 January 2025 | **Accepted:** 17 February 2025

Funding: This work was funded by the Australian Research Council Centre of Excellence for Integrative Brain Function (ARC Centre Grant CE140100007). KML received funding from the Lundbeck foundation (R322-2019-2311).

ABSTRACT

40 Hz auditory steady-state responses (ASSR) can be evoked by brief auditory clicks delivered at 40 Hz. While the neuropharmacology behind the generation of ASSR is well examined, the link between ASSR and microstructural properties of the brain is unclear. Further, whether the 40 Hz ASSR can be manipulated through processes involving top-down control, such as prediction, is currently unknown. We recorded EEG in 50 neurotypical participants while they engaged in a 40 Hz auditory steady-state paradigm. We manipulated the predictability of the stimuli to test the modulatory effect of prediction on 40 Hz steady-state responses. Further, we acquired T1w and T2w structural MRI on the same individuals and used the T1/T2 ratio as a proxy to determine myelination content in gray matter. The phase locking of the 40 Hz ASSR was indeed modulated by prediction, suggesting that prediction violation directly affects phase locking to the 40 Hz ASSR. We found that the prediction violation of the phase locking at 40 Hz (gamma) was associated with the degree of gray matter myelination in the right cerebellum, such that greater myelin led to less desynchronization induced by prediction violations. We demonstrate that prediction violations modulate steady-state activity at 40 Hz and suggest that the efficiency of this process is promoted by greater cerebellar myelin. Our findings provide a structural-functional relationship for myelin and phase locking of auditory oscillatory activity. These results introduce a framework for investigating the interaction of predictive processes and ASSR in disorders where these processes are impaired, such as in psychosis.

1 | Introduction

The generation of synchronous activity in the brain underpins coordinated activity and connectivity among functional networks. Consistent evidence shows that theta and gamma oscillations

propagate via feedforward connections, whereas beta and alpha oscillations propagate through backward connections (Bastos et al. 2015; Jensen et al. 2015; Van Kerkoerle et al. 2014). Given the role of oscillatory activity in enabling brain connectivity, the interplay between frequency bands may therefore enable

This is an open access article under the terms of the [Creative Commons Attribution-NonCommercial](https://creativecommons.org/licenses/by-nc/4.0/) License, which permits use, distribution and reproduction in any medium, provided the original work is properly cited and is not used for commercial purposes.

© 2025 The Author(s). *Human Brain Mapping* published by Wiley Periodicals LLC.

interplay between bottom-up and top-down processing. In fact, in the visual domain, beta activity enhances gamma activity (Richter et al. 2017) indicating an interplay between top-down and bottom-up processing. In this way, top-down control can enhance the ability to generate gamma oscillations.

One way to evoke cortical gamma oscillations is through exposure to auditory stimuli by brief tones or clicks at repetition rates of 40 Hz. In this way, an auditory steady-state response (ASSR) is elicited and can be measured with electroencephalography (EEG). These cortical gamma oscillations rely on the integrity of fast-spiking GABAergic interneurons, which exert a finely timed inhibition onto the pyramidal cells and other inhibitory interneurons (Bartos et al. 2007; Sohal et al. 2009; Traub et al. 2003). Both the phase and power of the ASSR are believed to reflect the inhibitory/excitatory balance mediated by the N-methyl-D-aspartate (NMDA) receptor (Sivarao et al. 2016; Tada et al. 2020). Evidence suggests that the ASSR is modulated by attention (Matulyte et al. 2024). For example, (Skosnik et al. 2007) found that when arranging click-trains in a classical oddball paradigm, selectively attending to target tones enhanced the ASSR compared to standard tones. While the 40 Hz ASSR can be modulated by attention, it is currently unknown whether this response can be modulated by other top-down processes (beyond attention) such as predictability. Detecting violations to those predictions, such as changes in the acoustic environment, is critical for survival, as these indicate potential threats or rewards (Friston 2005). A classic way to investigate this process in the controlled lab environment is to use a sequence of auditory streams of highly probable standard sounds and surprising deviant sounds that generate a mismatch response (Fitzgerald and Todd 2020). This is the so-called mismatch negativity (MMN) paradigm, where the mismatch negativity response is observed by subtracting the responses to the standard tones from the responses to the deviant tones. In this way, the standard tone will be perceived as a predictable tone, and the deviant tone will be perceived as the unpredictable or less predictable tone, and tones can thereby be compared with the modulation of predictability.

While neuropharmacological studies have linked ASSR to NMDA and GABA (Sivarao 2015; Sohal et al. 2009; Tada et al. 2020), the relationship between the expression of ASSR and microstructural properties of the brain is unclear. T1-weighted (T1w) and T2-weighted (T2w) images can be combined to assess tissue microstructure via T1w/T2w ratio maps (Ganzetti et al. 2014). Whole brain T1w/T2w ratio maps have provided a sensitive measure related to myelin and microstructural integrity in conditions such as multiple sclerosis (Beer et al. 2016) and schizophrenia (Ganzetti et al. 2015). Recently, gray matter myelin has been linked to electrophysiological functional connectivity (Hunt et al. 2016). Hunt et al. (2016) employed frequency-dependent functional connectivity to characterize the functional networks associated with different frequency bands. By comparing these frequency-dependent functional networks with structural connectivity derived from myelin maps, they identified the strongest correlation between myelin and functional networks to be in the beta and gamma frequency bands. Similarly, the rhythmicity of high-frequency oscillations is related to cortical myelin content (Tomasevic et al. 2022) and activity-dependent myelination has been shown to promote neural phase synchronization (Noori et al. 2020). Hence, there is increasing evidence that the microstructure of the cortex supports functional networks. The idea of myelin playing a role in the ability

to generate oscillatory synchrony becomes clear when noting that myelin speeds up conduction velocity (Dutta et al. 2018). In this way, even small changes in the conduction velocity can impact the generation of synchrony and coupling between brain regions (Pajevic et al. 2014). (Mancini et al. 2022) and (Kim et al. 2019) identified a correlation between 40 Hz ASSR power and auditory cortex volume, linking functional ASSR to cortical atrophy. However, it is still unknown if the power and phase locking of the ASSR scale with the degree of cortical myelination.

Disturbed interactions of the circuits underlying ASSR are thought to critically contribute to pathogenesis and cognitive impairment in neurodevelopmental disorders such as schizophrenia (Gonzalez-Burgos et al. 2011; Jadi et al. 2016; Thuné et al. 2016), bipolar disorder (Jefsen et al. 2022) as well as autism spectrum disorder (Arutiunian et al. 2023; Seymour et al. 2020; Wilson et al. 2007). Reduction in the 40 Hz ASSR is not only seen in chronic schizophrenia but also in first episode psychosis (Spencer et al. 2008; Symond et al. 2005), as well as in non-affected first-degree relatives (Hong et al. 2004; Rass et al. 2012). Given that both MMN (Umbricht and Krljes 2005) and 40 Hz ASSR (Thuné et al. 2016) are reduced in psychosis, introducing ASSR in a predictive setting will provide insights into how basic auditory processing and top-down network integration may go awry in these disorders.

Mounting evidence suggests that psychotic-like experiences occur to a certain extent in the healthy general population (Verdoux and van Os 2002) has led to the formulation of the continuum of psychosis hypothesis. According to this hypothesis, every individual in the general population lies somewhere on a continuum of psychotic-like traits, with some individuals scoring high on the personality dimension of schizotypy, i.e., psychotic-like experiences. Indeed, some of the behavioral, functional, and electrophysiological deficits seen in clinical psychosis are also observed to some extent in the healthy population; see for example (Dzafic et al. 2021; Jahshan et al. 2012; Oestreich et al. 2019, and Randeniya et al. 2018 for a review). However, how ASSR scales with psychotic-like experiences in individuals without a disorder is unknown.

Given the link between reduced ASSR and neurodevelopmental disorders, here we ask whether psychotic-like experiences in the general population are associated with inter-individual differences in ASSR. We introduce ASSR in a predictive setting integrating lower-level auditory processing with higher-level network processes. We ask whether 40 Hz ASSR can be manipulated by predictability (in a predictive versus unpredictable context) and whether these electrophysiological readouts are related to the degree of myelination.

2 | Methods

2.1 | Participants

Fifty healthy adults 18–25 years were recruited through the Psychology Research Participation Scheme (SONA) at the University of Queensland. Prior screening ruled out participants reporting a history of psychiatric or neurological disorders and currently on medication acting on the central nervous

system. Participants completed the 92 Item-Prodromal questionnaire (PQ), which measures positive and negative symptoms and is typically used to assess psychotic experiences in healthy individuals (Loewy et al. 2005). In addition, participants completed the Beck Depression questionnaire (Beck, Steer, et al. 1988) and Beck anxiety (Beck, Epstein, et al. 1988). To ensure that the PQ scores were not mainly driven by depressive or anxiety symptoms, participants meeting the threshold for moderate anxiety or depression were excluded. Participants provided written informed consent and received monetary reimbursement for their time. This research was approved by the University of Queensland Human Research Ethics.

2.2 | Paradigm

Participants were presented with a 40 Hz auditory steady-state paradigm with the 40 Hz click trains arranged in a traditional oddball paradigm, while we measured EEG (see Figure 1). In this way, it was possible to evoke 40 Hz gamma oscillations through click trains with the manipulation of expectancy of the tone. The sequence of tones/click trains was pseudo-randomly generated with a 20% probability for the deviant tone and an 80% probability for the standard tone. Click trains were presented with a stimulus onset asynchrony of 1.25 s and at a comfortable level. The design was divided into two blocks where deviant stimuli were longer than the standards in the long block and vice versa in the short block. This allowed us to compare the deviant stimuli from the long block to the standard stimuli of the short block, ensuring the comparison of stimuli with the same physical properties but with a change in expectancy of the tone duration (even though duration was matched). We divided each block into two runs of approximately 8 min, meaning that the total recording time was (4×8 min). This ensured that we had at least 150 trials for the deviant stimuli in each block (referred to as long and

short blocks in Figure 1) and approximately 600 trials for the standard stimuli in each block. Runs and blocks were counter-balanced across subjects. To keep participants engaged, they were asked to perform a visual 1-back task, which had participants detect repetitions of letters continuously presented and which did not coincide with the sounds.

2.3 | EEG and Preprocessing

EEG data were recorded using a 64-channel Biosemi active two, with electrodes arranged according to the 10–20 system and a sampling frequency of 1024 Hz. All offline preprocessing was performed using SPM 12 (<http://www.fil.ion.ucl.ac.uk/spm/>), which included high and low pass filtering with a 5th order Butterworth filter with a cutoff of 0.5 and 80 Hz, respectively. A notch filter was applied with cutoff of 48–52 Hz. Data were epoched with a peristimulus interval of –250–1000 ms, with baseline correction applied from –250 to 0 ms. Finally, artifact rejection was performed using a simple threshold technique, rejecting trials with amplitudes exceeding $\pm 100 \mu V$. Finally, the signals were referenced to the average of the two mastoid electrodes.

2.4 | Time-Frequency Analysis

The epoched data were wavelet-transformed using a Complex Morlet wavelet with 7 cycles and a frequency band of interest covering frequencies from 2 to 80 Hz at 1 Hz resolution. Power and phase-locking factor (PLF) were extracted from the wavelet coefficients. The amplitude of the PLF reflects the phase consistency across trials for a given channel, time, and frequency point. Values of PLF are bounded between 0 and 1, with 1 being perfect phase synchrony across trials. To compare power and PLF values for the different frequency bands, values were extracted during the time of stimulation 150–500 ms

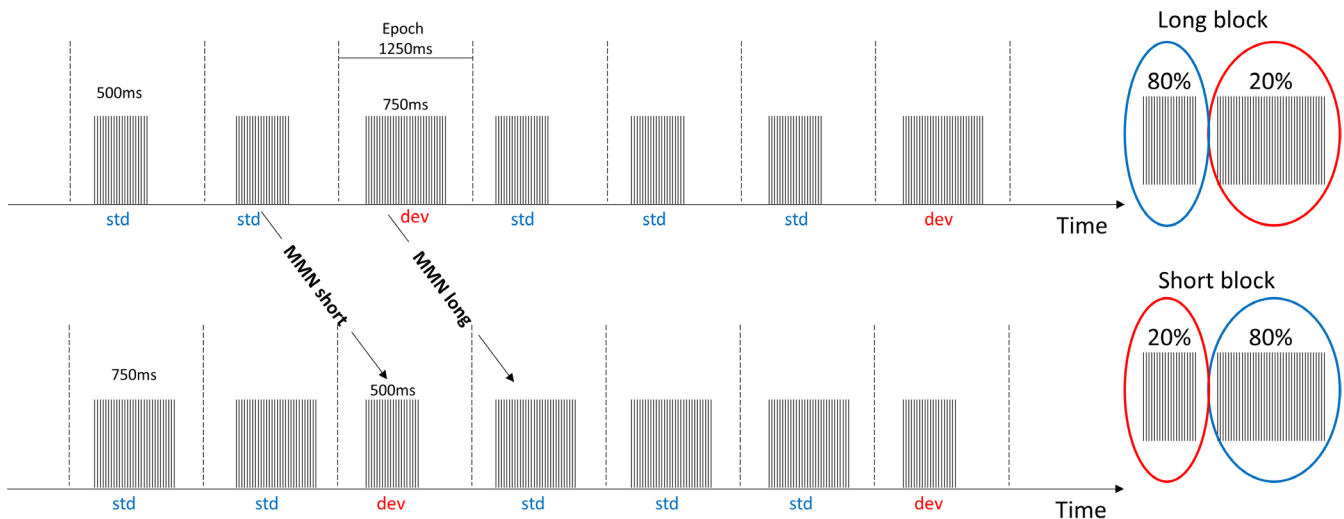


FIGURE 1 | Click trains with a frequency of 40 Hz were arranged in a classical oddball paradigm where the deviant changed tone duration to either be longer than the standard (long block) or shorter than the standard (short block). The MMN_{short} responses were derived by contrasting the standard tone in the long block with the deviant tone in the short block to ensure comparison of stimuli with the same duration. Likewise, the MMN_{long} responses were derived by contrasting the standard tone in the short block with the deviant stimuli in the long block. Epochs were extracted from 250 ms pre-stimulus to 1000 ms post-stimulus onset.

and for the standard frequency bands of theta (4–7 Hz), alpha (8–12 Hz), beta (15–25 Hz), and gamma (35–45 Hz). When applying time-frequency analysis with wavelets, some smoothing of the calculated responses is to be expected. We used 7 cycles in the wavelet to minimize this smoothing while still ensuring that we captured the full 40 Hz ASSR response with a window of 35–45 Hz, as used in prior studies (Holton et al. 2025; Parciauskaite et al. 2019; Sivarao et al. 2016). We analyze the whole data spectrum and show the spatial distribution of the effects on topographical plots. We then zoom in on data extracted from electrode Cz where 40 Hz ASSR typically shows the largest amplitude. To compare PLF and power values in the standard and deviant conditions, a two-sample *t*-test was performed. We performed both a traditional frequentist statistical approach reporting *p* values as well as a Bayesian approach reporting Bayes factors (BF_{10}). When multiple tests were performed, we used Bonferroni correction for all reported *p*-values. All statistical analyses were performed in R, using the packages ggpubr and BayesFactor.

2.5 | Approximation of Level of Myelination

To get an approximation for myelin content, a T1-weighted magnetization prepared rapid gradient-echo (MPRAGE) and a T2 SPACE sequence were acquired for all participants on a Siemens 3T Prisma scanner with a 64-channel head coil. T1-weighted data were acquired using the following parameters: Repetition time (TR)=4 s, echo time (TE)=29 ms, flip angle (FA)=6°, and an isotropic resolution of 1 mm with a matrix size=[176,240,256]. Similarly, T2-weighted data were acquired using TR=3.2 s, TE=0.408 s, TR=3.2, FA=120°, and a resolution of 1 mm isotropic with a matrix size=[176,256,256]. The T1w/T2w ratio maps were calculated using the MRtool integrated in SPM12 (Ganzetti et al. 2015, 2014). Preprocessing steps include bias correction, intensity normalization, and computation of the T1w/T2w ratio in the MNI space. We segmented T1w images into gray and white matter using the segmentation implemented in SPM12. Based on this segmentation, we extracted the T1w/T2w value of the gray matter regions. We focused on the gray matter, since this generates the ASSR (Farahani et al. 2021). Before using these in the GLMs, images were smoothed using a 4×4×4 mm kernel.

2.6 | Relationship Between EEG Measures and Degree of Myelination

To investigate the relationship between the power and phase-locking factor (PLF) of the different frequency bands of the EEG-evoked ASSR, we performed separate GLMs at the voxel level with the T1w/T2w ratio images as dependent variables. One GLM per measure (power and PLF) for the gray matter was performed with the EEG measure for each frequency band as regressors and age and gender as covariates. We further included total gray matter volume as a covariate to control for individual volume levels. All results are reported for surviving clusters corrected at $p < 0.05$ FWE, with a cluster forming threshold of $p < 0.001$ uncorrected. For significant clusters, we extracted the values of the T1w/T2w images in a

10 mm square around the peak coordinate of the cluster. This extraction was performed to visualize the intensity values and the EEG measures.

3 | Results

Three participants were excluded due to scores reaching thresholds for severe anxiety or moderate depression on the Becks inventories. Additionally, two participants were excluded due to very noisy EEG data, resulting in 45 participants in the main analyses (mean age 21.32 ± 1.97 , 27 females, 18 males). PQ scores were distributed between 5 and 128, with a mean of 55.6 ± 31.5 .

3.1 | Phase Locking Across Trials Is Modulated by Prediction in the Gamma Band

To test if predictability can modulate power and phase locking across trials, we compared the responses for standard and deviant stimuli in the gamma band (see upper row of Figure 2A for power and lower row for PLF). Indeed, phase locking to the stimulus across trials was modulated by sound predictability in the gamma band, indicated by an increase in PLF for deviant trials compared to standard trials (see time-frequency plot in Figure 2 for the long blocks). Overall, there were no differences between long and short blocks; therefore, the figures show the long block and we have pooled the data across long and short blocks when reporting the statistical findings. Since this increase in the PLF seems to also be present in the pre-stimulus interval, we corrected all extracted values with the values observed in the pre-stimulus interval; see Figure 3.

Extracting values of PLF, showed a robust difference between the standard and deviant trials, consistent across participants, (see Figure 3) with extracted values from channel Cz (where peak amplitudes for the 40 Hz ASSR are usually observed, see topography in Figure S1). In fact, correcting for the baseline values in the 40 Hz gamma band, revealed that the PLF is decreased in the 40 Hz gamma band for the deviant stimuli compared to the standard stimuli ($p < 0.001$ $BF_{10} > 100$). There was no effect of prediction on the power of the 40 Hz ASSR ($p = 0.823$, $BF_{10} = 0.166$). To assess if this decrease in phase-locking value was specific to the gamma band and thereby related to the frequency band of stimulation, we tested for differences in the theta, alpha, and beta band as well ($p_{\text{theta}} = 0.539$, $BF_{10 \text{ theta}} = 0.194$, $p_{\text{alpha}} = 0.085$, $BF_{10 \text{ alpha}} = 2.059$, $p_{\text{beta}} = 0.969$, $BF_{10 \text{ beta}} = 0.162$). Indeed, the modulation of prediction was only present for the gamma band. The power for the remaining frequency bands revealed a significant effect for the theta band ($p_{\text{theta}} = 0.006$, $BF_{10 \text{ theta}} = 20.079$, $p_{\text{alpha}} = 0.850$, $BF_{10 \text{ alpha}} = 0.164$, $p_{\text{beta}} = 0.158$, $BF_{10 \text{ beta}} = 1.237$), and no effect of the other bands.

3.2 | Forty Hertz Phase Locking of ASSR Increases With Greater Myelin Content

Since ASSR is generated in the gray matter, we performed a GLM using the gray matter T1w/T2w intensity images (Farahani et al. 2021). The difference in PLF between the standard and deviant was positively associated with myelin content in the right

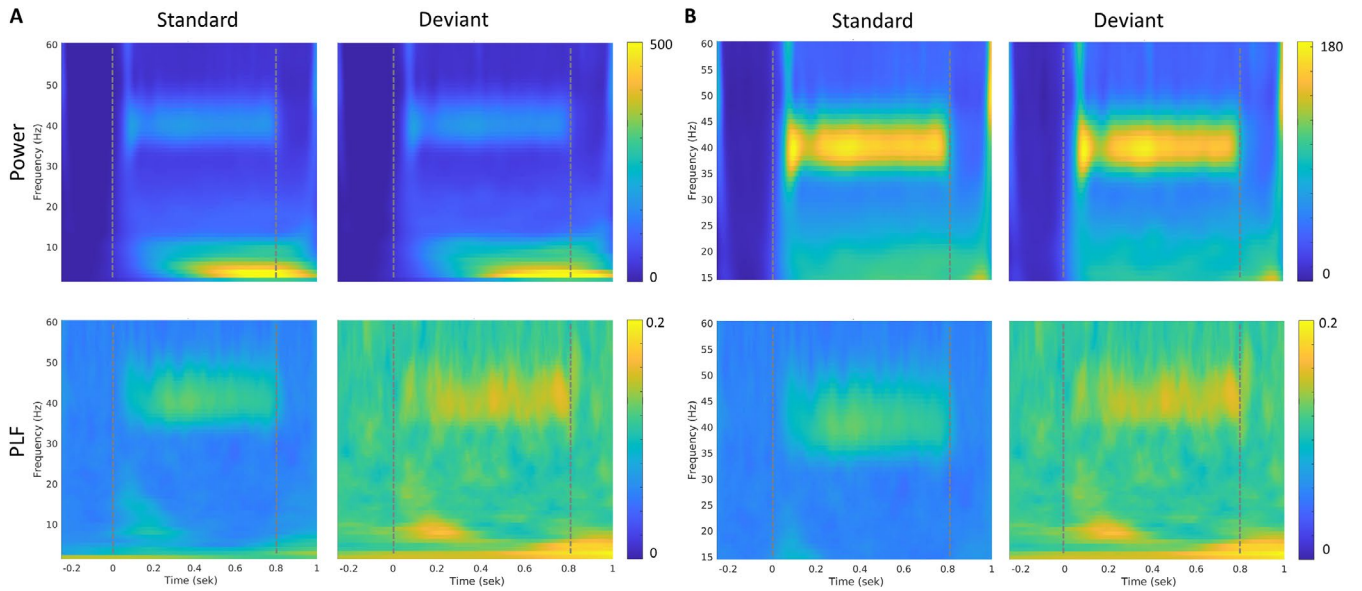


FIGURE 2 | Time-frequency responses at channel Cz averaged across participants (for the long block, similar findings in the short block, see sup Figure 2). Dotted lines indicate onset and offset of auditory stimuli. (A) Full frequency spectrum covering 2–60 Hz. (B) Zoomed in at 15–60 Hz to highlight the successful evoking of 40 Hz.

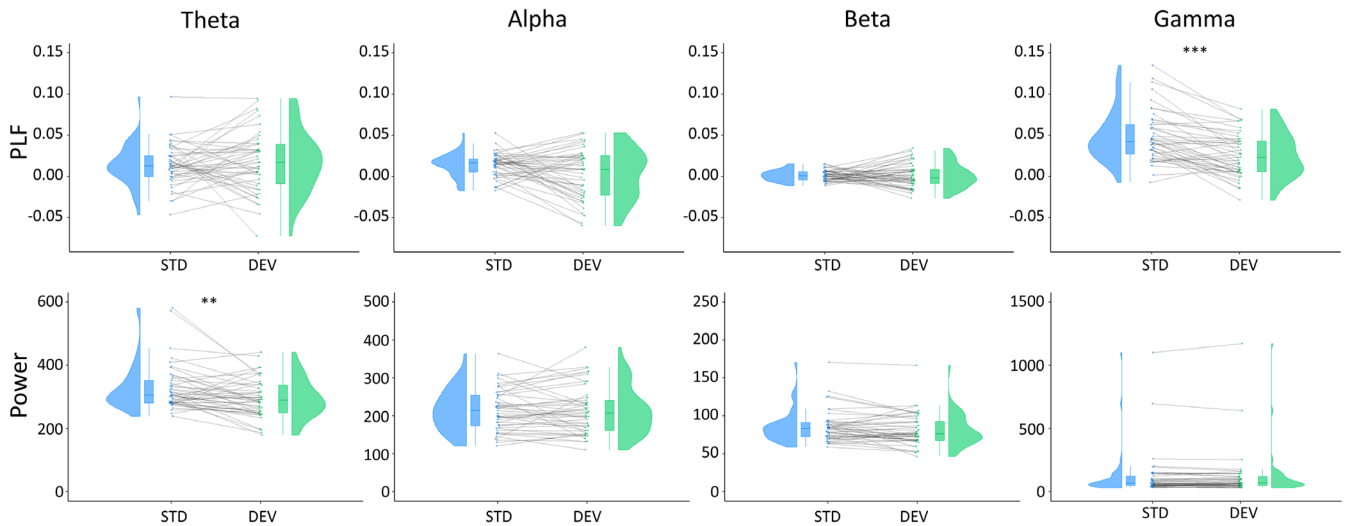


FIGURE 3 | Power (bottom) and phase-locking factor (top) extracted from channel Cz in the period of stimulation averaged across the long and short blocks. Blue indicates standard and green is deviant. The connecting gray line indicates the relationship between the standard and deviant for each individual participant. ** is $p < 0.01$, *** is $p < 0.001$, corrected for multiple comparison.

cerebellum (Crus I), with peak values in [MNI 53 –57 –34] (see Figure 4A). This was such that the greater the myelin content, the less the neural responses became desynchronized by the deviant. Figure 4B shows the extracted T1w/T2w intensities in the significant cluster together with the phase-locking values (difference between standard and deviant). The individual levels of phase-locking values for the standard and deviant alone in the gamma band, however, did not correlate with the T1/T2 intensities.

3.3 | No Evidence That 40 Hz ASSR Is Correlated With Psychotic-Like Experiences

There was no correlation between the amount of gamma oscillation power and the degree of psychotic-like experiences (deviant

responses $p = 0.827$, $BF_{10} = 0.341$, standard responses $p = 0.860$, $BF_{10} = 0.339$). The same was the case for the PLF and psychotic-like experiences (deviant responses $p = 0.763$, $BF_{10} = 0.348$, standard responses $p = 0.268$, $BF_{10} = 0.578$).

4 | Discussion

Here, we show that the ability to generate synchronous activity in the 40 Hz range through ASSRs can be modulated by prediction. This modulation of prediction on the phase locking of the ASSR was linked to the myelin content in the gray matter of the cerebellum, potentially suggesting a mechanism for the ability to generate synchronous neural activity. Contrary to our hypothesis, we did not find any association

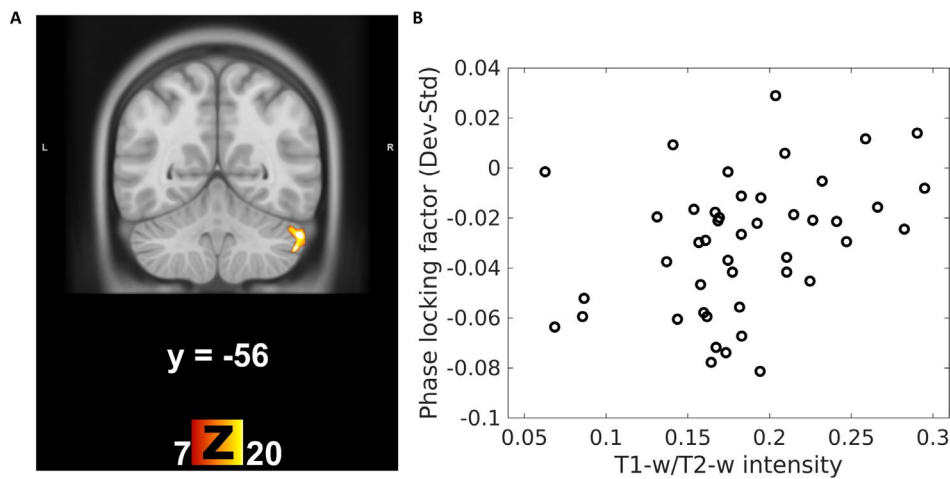


FIGURE 4 | (A) Association between myelin content and phase-locking for the gamma band (between the standard and deviant). Peak of the association was found in MNI coordinates [53 -57 -34]. Cluster forming threshold was set to $p=0.001$ uncorrected, and results here only show the cluster that survived correction at the cluster level at $p<0.05$. (B) T1w/T2w intensity values extracted from the cluster in the cerebellum increase with the phase-locking factor of the difference wave (between the standards and deviants).

between the gamma range and the degree of psychotic-like experiences.

4.1 | ASSR Is Modulated by Prediction and Supports a Structure–Function Relationship

The violation of prediction induced by the oddball paradigm modulated the synchronization elicited by the 40 Hz stimulation, as indicated by lower phase-locking values for deviant responses compared to standard responses. We asked whether this desynchrony was associated with the degree of myelination. We found that prediction-error-based modulations of the oscillatory activations to 40 Hz auditory inputs were positively associated with cortical myelination in the right cerebellum, specifically the right Crus I, such that less desynchronization was induced by the deviant for greater cerebellum myelin content. The cortical generator of the ASSR is in the primary auditory cortex (temporal regions) (Arutiunian et al. 2022; Farahani et al. 2021), typically with a right hemisphere dominance (Kumar et al. 2023; Sugiyama et al. 2023). Further, the phase-locking value of the 40 Hz ASSR has sources in the frontal and parietal cortex (Tada et al. 2021). Although the auditory cortex is the primary generator of the 40 Hz ASSR, the Crus I/II of the cerebellum, i.e., the auditory cerebellum, is a key node in a distributed network involved in regulating the 40 Hz ASSR (Pastor et al. 2008, 2006, 2002). For example, ASSR amplitudes diminish after inhibitory transcranial magnetic stimulation over this area (Pastor et al. 2006). A high level of myelination in the cerebellum may enhance ASSR network synchronization and thus boost phase-locking values or mitigate desynchronization as in the current study. Additionally, it has been shown that the cerebellum mediates various perceptual and cognitive processes through its “predictive function” (Ivry and Fiez 2000). Specifically, the cerebellum likely tracks and predicts the timing of auditory events and recalibrates its temporal predictions in detecting incongruities between expected and perceived sensory inputs (Moberget et al. 2008; Kotz et al. 2014). Therefore, the degree of myelination in the Crus I/II may affect the ability to precisely encode temporal events and proactively reset temporal

predictions in response to prediction violation. Our finding of an association between oscillatory activity and myelin exclusively in the right hemisphere was unexpected and requires replication in a larger sample. While the 40 Hz ASSR responses are typically stronger in the right hemisphere (Kumar et al. 2023; Sugiyama et al. 2023), the evidence predominantly indicates that the Crus I is connected to the contralateral auditory cortex in the temporal lobe (Ren et al. 2021; Sokolov et al. 2014). Hence, if any lateralization, we would have expected a stronger effect on the left, rather than on the right cerebellum.

Interestingly, we showed that the association between oscillatory activity and cortical myelination was only present for the phase locking and not the magnitude of the 40 Hz oscillatory activity. Similar results have recently been found using somatosensory stimulation (Tomasevic et al. 2022). They showed that the rhythmicity of high-frequency oscillations within the human sensorimotor cortex was related to the cortical myelin content in the primary sensory area. Consistent with our findings, this association was only found for the rhythmicity and not the magnitude of the frequency content. Given the role of myelin in conducting velocity, even small changes in myelin can cause changes to the phase of the signal propagation (Pajevic et al. 2014). The modulation of prediction was additionally significant in the power of the theta band, whereas the phase-locking value in the theta band did not differ between standard and deviant responses. The power of the theta band is known to be involved in the generation of the mismatch negativity response (Javitt et al. 2018; Hua et al. 2023). While the tendency in traditional oddball paradigms, not including ASSR, is that theta increases for deviant responses, we found this to decrease when controlling for baseline values. This could be due to the coupling of the theta and gamma oscillations (Lisman and Jensen 2013); however, this warrants replication in a study with a specific focus on this question.

A limitation of the current study is that the T1w/T2w map is sensitive to the cortical myelin content (Ganzetti et al. 2014; Glasser and van Essen 2011) and thereby not a direct quantitative measure of myelin. This is a limitation when comparing between

studies with different scanning parameters, which can have an impact on the approximation of myelin content. When interpreting findings from images acquired using the T1/T2 ratio as an approximation of myelin content, one should be aware that artifacts can appear in regions very close to air and tissue interfaces (Glasser and van Essen 2011).

4.2 | No Evidence That 40 Hz ASSR Is Correlated With PQ

Inspired by the idea of the continuum of psychosis (Van Os et al. 2009), we hypothesized that the 40 Hz ASSR would scale with the degree of psychotic-like experiences. However, our data did not support this hypothesis, with the Bayes factors showing anecdotal evidence against a relationship. While 40 Hz ASSR is reduced in first-degree relatives (Hong et al. 2004; Rass et al. 2012; Thuné et al. 2016) and in individuals at clinical (Grent-‘t-Jong et al. 2021) or genetic (Larsen et al. 2018) high risk for psychosis, no study to date has looked at this in healthy individuals assessed for PLE. We note that the participants included here were in the lower range of the PQ scale ranging from 5 to 128 with a mean of 55.6 ± 31.5 . Although we attempted to have a wide range of psychotic-like experiences, some participants scoring higher on the PQ scale also scored high on either the Beck anxiety or depression inventory and therefore were not included in the study, hence reducing the sample size and the spread of severity of psychotic-like experiences. As non-clinical trait effects are often rather small, future studies would benefit from using a wider spread of psychotic-like experiences in a larger sample, where factors such as anxiety and depression traits can be regressed out. An additional scope for future studies is to investigate whether predictable versus unpredictable contexts modulate phase locking of the 40 Hz ASSR in people with psychosis as well as how the structure–function relationship is affected.

5 | Conclusion

The current study introduces a novel combination of 40 Hz ASSR with a classical oddball paradigm. This paradigm introduces the possibility to examine both predictive processes and entrained oscillatory activity in the lower gamma range. In addition, it offers the possibility to study the interaction between the two. We show that the generation of synchronous neural activity in the lower gamma range is linked to the degree of myelination in the right cerebellum. Therefore, our results confirm that the microstructure of the cortex supports functional networks.

Acknowledgments

We would like to thank all participants in this study for their time as well as the radiographers at the University of Queensland, Mr. Aiman Al-Najjar and Ms. Nicole Atcheson. This work was funded by the Australian Research Council Centre of Excellence for Integrative Brain Function (ARC Centre Grant CE140100007). K.M.L. received funding from the Lundbeck foundation (R322-2019-2311). Open access publishing facilitated by The University of Queensland, as part of the Wiley - The University of Queensland agreement via the Council of Australian University Librarians.

Ethics Statement

Participants provided written informed consent and received monetary reimbursement for their time. This research was approved by the University of Queensland Human Research Ethics Committee.

Conflicts of Interest

H.R.S. has received honoraria as a speaker from Sanofi Genzyme, Denmark, and Novartis, Denmark; as a consultant from Sanofi Genzyme, Denmark; and as senior editor (NeuroImage) and editor-in-chief (Neuroimage Clinical) from Elsevier Publishers, Amsterdam, The Netherlands. H.R.S. has also received royalties as book editor from Springer Publishers, Stuttgart, Germany, and Gyldendahl Publishers, Copenhagen, Denmark. All disclosures are independent of the work published here. All other authors declare no conflicts of interest.

Data Availability Statement

The data that support the findings of this study are available from the corresponding author upon reasonable request.

References

- Arutunian, V., G. Arcara, I. Buyanova, et al. 2023. “Neuromagnetic 40 Hz Auditory Steady-State Response in the Left Auditory Cortex Is Related to Language Comprehension in Children With Autism Spectrum Disorder.” *Progress in Neuro-Psychopharmacology & Biological Psychiatry* 122: 110690. <https://doi.org/10.1016/J.PNPBP.2022.110690>.
- Arutunian, V., G. Arcara, I. Buyanova, M. Gomozya, and O. Dragoy. 2022. “The Age-Related Changes in 40 Hz Auditory Steady-State Response and Sustained Event-Related Fields to the Same Amplitude-Modulated Tones in Typically Developing Children: A Magnetoencephalography Study.” *Human Brain Mapping* 43: 5370–5383. <https://doi.org/10.1002/HBM.26013>.
- Bartos, M., I. Vida, and P. Jonas. 2007. “Synaptic Mechanisms of Synchronized Gamma Oscillations in Inhibitory Interneuron Networks.” *Nature Reviews. Neuroscience* 8: 45–56. <https://doi.org/10.1038/nrn2044>.
- Bastos, A. M., J. Vezoli, C. A. Bosman, et al. 2015. “Visual Areas Exert Feedforward and Feedback Influences Through Distinct Frequency Channels.” *Neuron* 85: 390–401. <https://doi.org/10.1016/j.neuron.2014.12.018>.
- Beck, A. T., N. Epstein, G. Brown, and R. A. Steer. 1988. “An Inventory for Measuring Clinical Anxiety: Psychometric Properties.” *Journal of Consulting and Clinical Psychology* 56: 893–897. <https://doi.org/10.1037/0022-006X.56.6.893>.
- Beck, A. T., R. A. Steer, and M. G. Carbin. 1988. “Psychometric Properties of the Beck Depression Inventory: Twenty-Five Years of Evaluation.” *Clinical Psychology Review* 8: 77–100. [https://doi.org/10.1016/0272-7358\(88\)90050-5](https://doi.org/10.1016/0272-7358(88)90050-5).
- Beer, A., V. Biberacher, P. Schmidt, et al. 2016. “Tissue Damage Within Normal Appearing White Matter in Early Multiple Sclerosis: Assessment by the Ratio of T1- and T2-Weighted MR Image Intensity.” *Journal of Neurology* 263: 1495–1502. <https://doi.org/10.1007/S00415-016-8156-6>.
- Dutta, D. J., D. H. Woo, P. R. Lee, et al. 2018. “Regulation of Myelin Structure and Conduction Velocity by Perinodal Astrocytes.” *Proceedings of the National Academy of Sciences of the United States of America* 115: 11832–11837. <https://doi.org/10.1073/PNAS.1811013115>.
- Dzafic, I., K. M. Larsen, H. Darke, et al. 2021. “Stronger Top-Down and Weaker Bottom-Up Frontotemporal Connections During Sensory Learning Are Associated With Severity of Psychotic Phenomena.” *Schizophrenia Bulletin* 47: 1039–1047. <https://doi.org/10.1093/SCHBUL/SBAA188>.

- Farahani, E. D., J. Wouters, and A. van Wieringen. 2021. "Brain Mapping of Auditory Steady-State Responses: A Broad View of Cortical and Subcortical Sources." *Human Brain Mapping* 42: 780–796. <https://doi.org/10.1002/HBM.25262>.
- Fitzgerald, K., and J. Todd. 2020. "Making Sense of Mismatch Negativity." *Frontiers in Psychiatry* 11: 468. <https://doi.org/10.3389/FPSYT.2020.00468/BIBTEX>.
- Friston, K. 2005. "A Theory of Cortical Responses." *Philosophical Transactions of the Royal Society of London. Series B, Biological Sciences* 360: 815–836. <https://doi.org/10.1098/rstb.2005.1622>.
- Ganzetti, M., N. Wenderoth, and D. Mantini. 2014. "Whole Brain Myelin Mapping Using T1- and T2-Weighted MR Imaging Data." *Frontiers in Human Neuroscience* 8. <https://doi.org/10.3389/fnhum.2014.00671>.
- Ganzetti, M., N. Wenderoth, and D. Mantini. 2015. "Mapping Pathological Changes in Brain Structure by Combining T1- and T2-Weighted MR Imaging Data." *Neuroradiology* 57: 917–928. <https://doi.org/10.1007/S00234-015-1550-4>.
- Glasser, M. F., and D. C. van Essen. 2011. "Mapping Human Cortical Areas In Vivo Based on Myelin Content as Revealed by T1- and T2-Weighted MRI." *Journal of Neuroscience* 31: 11597–11616. <https://doi.org/10.1523/JNEUROSCI.2180-11.2011>.
- Gonzalez-Burgos, G., K. N. Fish, D. A. Lewis, G. Gonzalez-Burgos, K. N. Fish, and D. A. Lewis. 2011. "GABA Neuron Alterations, Cortical Circuit Dysfunction and Cognitive Deficits in Schizophrenia." *Neural Plasticity* 2011: 723184. <https://doi.org/10.1155/2011/723184>.
- Grent-‘t-Jong, T., R. Gajwani, J. Gross, et al. 2021. "40-Hz Auditory Steady-State Responses Characterize Circuit Dysfunctions and Predict Clinical Outcomes in Clinical High-Risk for Psychosis Participants: A Magnetoencephalography Study." *Biological Psychiatry* 90: 419–429. <https://doi.org/10.1016/J.BIOPSYCH.2021.03.018>.
- Holton, K. M., A. Higgins, A. J. Brockmeier, and M. H. Hall. 2025. "Uncovering Key Predictive Channels and Clinical Variables in the Gamma Band Auditory Steady-State Response in Early-Stage Psychosis: A Longitudinal Study." *Acta Neuropsychiatrica* 37: e1. <https://doi.org/10.1017/NEU.2024.60>.
- Hong, L. E., A. Summerfelt, R. McMahon, et al. 2004. "Evoked Gamma Band Synchronization and the Liability for Schizophrenia." *Schizophrenia Research* 70: 293–302. <https://doi.org/10.1016/j.schres.2003.12.011>.
- Hua, J. P. Y., B. J. Roach, J. M. Ford, and D. H. Mathalon. 2023. "Mismatch Negativity and Theta Oscillations Evoked by Auditory Deviance in Early Schizophrenia." *Biological Psychiatry: Cognitive Neuroscience and Neuroimaging* 8: 1186–1196. <https://doi.org/10.1016/J.BPSC.2023.03.004>.
- Hunt, B. A. E., P. K. Tewarie, O. E. Mougin, et al. 2016. "Relationships Between Cortical Myeloarchitecture and Electrophysiological Networks." *Proceedings of the National Academy of Sciences of the United States of America* 113: 13510–13515. <https://doi.org/10.1073/pnas.1608587113>.
- Ivry, R., and J. Fiez. 2000. *The New Cognitive Neurosciences*. Second ed. MIT Press.
- Jadi, M. P., M. M. Behrens, T. J. Sejnowski, et al. 2016. "Abnormal Gamma Oscillations in N-Methyl-D-Aspartate Receptor Hypofunction Models of Schizophrenia." *Biological Psychiatry* 79: 716–726. <https://doi.org/10.1016/j.biopsych.2015.07.005>.
- Jahshan, C., K. S. Cadenhead, A. J. Rissling, K. Kirihaara, D. L. Braff, and G. A. Light. 2012. "Automatic Sensory Information Processing Abnormalities Across the Illness Course of Schizophrenia." *Psychological Medicine* 42: 85–97. <https://doi.org/10.1017/S0033291711001061>.
- Javitt, D. C., M. Lee, J. T. Kantrowitz, and A. Martinez. 2018. "Mismatch Negativity as a Biomarker of Theta Band Oscillatory Dysfunction in Schizophrenia." *Schizophrenia Research* 191: 51–60. <https://doi.org/10.1016/J.SCHRES.2017.06.023>.
- Jefsen, O. H., Y. Shtyrov, K. M. Larsen, and M. J. Dietz. 2022. "The 40-Hz Auditory Steady-State Response in Bipolar Disorder: A Meta-Analysis." *Clinical Neurophysiology* 141: 53–61. <https://doi.org/10.1016/J.CLINPH.2022.06.014>.
- Jensen, O., M. Bonnefond, T. R. Marshall, and P. Tiesinga. 2015. "Oscillatory Mechanisms of Feedforward and Feedback Visual Processing." *Trends in Cognitive Sciences* 38: 192–194. <https://doi.org/10.1016/j.tins.2015.02.006>.
- Kim, S., S. K. Jang, D. W. Kim, et al. 2019. "Cortical Volume and 40-Hz Auditory Steady-State Responses in Patients With Schizophrenia and Healthy Controls." *NeuroImage: Clinical* 22: 101732. <https://doi.org/10.1016/J.NICL.2019.101732>.
- Kotz, S. A., A. Stockert, and M. Schwartz. 2014. "Cerebellum, Temporal Predictability and the Updating of a Mental Model." *Philosophical Transactions of the Royal Society of London. Series B, Biological Sciences* 369: 20130403. <https://doi.org/10.1098/RSTB.2013.0403>.
- Kumar, N., A. Jaiswal, D. Roy, and A. Banerjee. 2023. "Effective Networks Mediate Right Hemispheric Dominance of Human 40 Hz Auditory Steady-State Response." *Neuropsychologia* 184: 108559. <https://doi.org/10.1016/J.NEUROPSYCHOLOGIA.2023.108559>.
- Larsen, K. M., G. Pellegrino, M. R. Birknow, et al. 2018. "22q11.2 Deletion Syndrome Is Associated With Impaired Auditory Steady-State Gamma Response." *Schizophrenia Bulletin* 44: 388–397. <https://doi.org/10.1093/schbul/sbx058>.
- Lisman, E., and O. Jensen. 2013. "The Theta-Gamma Neural Code." *Neuron* 77: 1002–1016. <https://doi.org/10.1016/J.NEURON.2013.03.007>.
- Loewy, L., C. E. Bearden, J. K. Johnson, A. Raine, and T. D. Cannon. 2005. "The Prodromal Questionnaire (PQ): Preliminary Validation of a Self-Report Screening Measure for Prodromal and Psychotic Syndromes." *Schizophrenia Research* 79: 117–125. <https://doi.org/10.1016/J.SCHRES.2005.03.007>.
- Mancini, V., V. Rochas, M. Seeber, et al. 2022. "Aberrant Developmental Patterns of Gamma-Band Response and Long-Range Communication Disruption in Youths With 22q11.2 Deletion Syndrome." *American Journal of Psychiatry* 179: 204–215. <https://doi.org/10.1176/APPI.AJP.2021.21020190>.
- Matulyte, G., V. Parciauskaite, J. Bjekic, E. Pipinis, and I. Griskova-Bulanova. 2024. "Gamma-Band Auditory Steady-State Response and Attention: A Systemic Review." *Brain Sciences* 14: 857. <https://doi.org/10.3390/BRAINSCI14090857>.
- Moberget, T., C. M. Karns, L. Y. Deouell, M. Lindgren, R. T. Knight, and R. B. Ivry. 2008. "Detecting Violations of Sensory Expectancies Following Cerebellar Degeneration: A Mismatch Negativity Study." *Neuropsychologia* 46: 2569–2579. <https://doi.org/10.1016/J.NEUROPSYCHOLOGIA.2008.03.016>.
- Noori, R., D. Park, J. D. Griffiths, et al. 2020. "Activity-Dependent Myelination: A Glial Mechanism of Oscillatory Self-Organization in Large-Scale Brain Networks." *Proceedings of the National Academy of Sciences of the United States of America* 117: 13227–13237. <https://doi.org/10.1073/PNAS.1916646117>.
- Oestreich, L. K. L., R. Randeniya, and M. I. Garrido. 2019. "White Matter Connectivity Reductions in the Pre-Clinical Continuum of Psychosis: A Connectome Study." *Human Brain Mapping* 40: 529–537. <https://doi.org/10.1002/HBM.24392>.
- Pajevic, S., P. J. Basser, and R. D. Fields. 2014. "Role of Myelin Plasticity in Oscillations and Synchrony of Neuronal Activity." *Neuroscience* 276: 135–147. <https://doi.org/10.1016/j.neuroscience.2013.11.007>.
- Parciauskaite, V., A. Voicikas, V. Jurkuvenas, et al. 2019. "40-Hz Auditory Steady-State Responses and the Complex Information Processing: An Exploratory Study in Healthy Young Males." *PLoS One* 14: e0223127. <https://doi.org/10.1371/JOURNAL.PONE.0223127>.

- Pastor, M. A., C. Vidaurre, M. A. Fernández-Seara, A. Villanueva, and K. J. Friston. 2008. "Frequency-Specific Coupling in the Cortico-Cerebellar Auditory System." *Journal of Neurophysiology* 100: 1699–1705. <https://doi.org/10.1152/JN.01156.2007>.
- Pastor, M. A., G. Thut, and A. Pascual-Leone. 2006. "Modulation of Steady-State Auditory Evoked Potentials by Cerebellar rTMS." *Experimental Brain Research* 175: 702–709. <https://doi.org/10.1007/S00221-006-0588-2>.
- Pastor, M. A., J. Artieda, J. Arbizu, J. M. Marti-Climent, I. Pañuelas, and J. C. Masdeu. 2002. "Activation of Human Cerebral and Cerebellar Cortex by Auditory Stimulation at 40 Hz." *Journal of Neuroscience* 22: 10501–10506. <https://doi.org/10.1523/JNEUROSCI.22-23-10501.2002>.
- Randeniya, R., L. K. L. Oestreich, and M. I. Garrido. 2018. "Sensory Prediction Errors in the Continuum of Psychosis." *Schizophr Res* 191: 109–122. <https://doi.org/10.1016/j.schres.2017.04.019>.
- Rass, O., J. K. Forsyth, G. P. Krishnan, et al. 2012. "Auditory Steady State Response in the Schizophrenia, First-Degree Relatives, and Schizotypal Personality Disorder." *Schizophrenia Research* 136: 143–149. <https://doi.org/10.1016/j.schres.2012.01.003>.
- Ren, J., C. S. Hubbard, J. Ahveninen, et al. 2021. "Dissociable Auditory Cortico-Cerebellar Pathways in the Human Brain Estimated by Intrinsic Functional Connectivity." In *Cerebral Cortex*, 2898–2912. Oxford University Press. <https://doi.org/10.1093/CERCOR/BHAA398>.
- Richter, C. G., W. H. Thompson, C. A. Bosman, and P. Fries. 2017. "Top-Down Beta Enhances Bottom-Up Gamma." *Journal of Neuroscience* 37: 6698–6711. <https://doi.org/10.1523/JNEUROSCI.3771-16.2017>.
- Seymour, R. A., G. Rippon, G. Gooding-Williams, P. F. Sowman, and K. Kessler. 2020. "Reduced Auditory Steady State Responses in Autism Spectrum Disorder." *Molecular Autism* 11: 1–13. <https://doi.org/10.1186/S13229-020-00357-Y/FIGURES/7>.
- Sivarao, D. V. 2015. "The 40-Hz Auditory Steady-State Response a Selective Biomarker for Cortical NMDA Function." *Annals of the New York Academy of Sciences* 1344: 27–36. <https://doi.org/10.1111/nyas.12739>.
- Sivarao, D. V., P. Chen, A. Senapati, et al. 2016. "40 Hz Auditory Steady-State Response Is a Pharmacodynamic Biomarker for Cortical NMDA Receptors." *Neuropsychopharmacology* 41: 2232–2240. <https://doi.org/10.1038/npp.2016.17>.
- Skosnik, P. D., G. P. Krishnan, and B. F. O'Donnell. 2007. "The Effect of Selective Attention on the Gamma-Band Auditory Steady-State Response." *Neuroscience Letters* 420: 223–228. <https://doi.org/10.1016/J.NEULET.2007.04.072>.
- Sohal, V. S., F. Zhang, O. Yizhar, and K. Deisseroth. 2009. "Parvalbumin Neurons and Gamma Rhythms Enhance Cortical Circuit Performance." *Nature* 459: 698–702. <https://doi.org/10.1038/nature07991>.
- Sokolov, A. A., M. Erb, W. Grodd, and M. A. Pavlova. 2014. "Structural Loop Between the Cerebellum and the Superior Temporal Sulcus: Evidence From Diffusion Tensor Imaging." *Cerebral Cortex* 24: 626–632. <https://doi.org/10.1093/CERCOR/BHS346>.
- Spencer, K. M., D. F. Salisbury, M. E. Shenton, and R. W. McCarley. 2008. "γ-Band Auditory Steady-State Responses Are Impaired in First Episode Psychosis." *Biological Psychiatry* 64: 369–375. <https://doi.org/10.1016/j.biopsych.2008.02.021>.
- Sugiyama, S., T. Taniguchi, T. Kinukawa, et al. 2023. "The 40-Hz Auditory Steady-State Response Enhanced by Beta-Band Subharmonics." *Frontiers in Neuroscience* 17: 1127040. <https://doi.org/10.3389/FNINS.2023.1127040/BIBTEX>.
- Symond, M. P., M. B. Symond, A. W. F. Harris, E. Gordon, and L. M. Williams. 2005. "Gamma Synchrony in First-Episode Schizophrenia: A Disorder of Temporal Connectivity?" *American Journal of Psychiatry* 162: 459–465. <https://doi.org/10.1176/appi.ajp.162.3.459>.
- Tada, M., K. Kirihaara, D. Koshiyama, et al. 2020. "Gamma-Band Auditory Steady-State Response as a Neurophysiological Marker for Excitation and Inhibition Balance: A Review for Understanding Schizophrenia and Other Neuropsychiatric Disorders." *Clinical EEG and Neuroscience* 51: 234–243. <https://doi.org/10.1177/1550059419868872>.
- Tada, M., K. Kirihaara, Y. Ishishita, et al. 2021. "Global and Parallel Cortical Processing Based on Auditory Gamma Oscillatory Responses in Humans." *Cerebral Cortex* 31: 4518–4532. <https://doi.org/10.1093/CERCOR/BHAB103>.
- Thuné, H., M. Recasens, and P. J. Uhlhaas. 2016. "The 40-Hz Auditory Steady-State Response in Patients With Schizophrenia: A Meta-Analysis." *JAMA Psychiatry* 73: 1145. <https://doi.org/10.1001/jamapsychiatry.2016.2619>.
- Tomasevic, L., H. R. Siebner, A. Thielscher, F. Manganeli, G. Pontillo, and R. Dubbioso. 2022. "Relationship Between High-Frequency Activity in the Cortical Sensory and the Motor Hand Areas, and Their Myelin Content." *Brain Stimulation* 15: 717–726. <https://doi.org/10.1016/J.BRS.2022.04.018>.
- Traub, R. D., M. O. Cunningham, T. Gloveli, et al. 2003. "GABA-Enhanced Collective Behavior in Neuronal Axons Underlies Persistent Gamma-Frequency Oscillations." *Proceedings of the National Academy of Sciences of the United States of America* 100: 11047–11052. <https://doi.org/10.1073/pnas.1934854100>.
- Umbricht, D., and S. Krljes. 2005. "Mismatch Negativity in Schizophrenia: A Meta-Analysis." *Schizophrenia Research* 76: 1–23. <https://doi.org/10.1016/j.schres.2004.12.002>.
- Van Kerkoerle, T., M. W. Self, and B. Dagnino. 2014. "Alpha and Gamma Oscillations Characterize Feedback and Feedforward Processing in Monkey Visual Cortex." *Proceedings of the National Academy of Sciences* 111: 14332–14341. <https://doi.org/10.1073/pnas.1402773111/-/DCSupplemental>.
- Van Os, J., R. J. Linscott, I. Myin-Germeys, P. Delespaul, and L. Krabbendam. 2009. "A Systematic Review and Meta-Analysis of the Psychosis Continuum: Evidence for a Psychosis Proneness–Persistence–Impairment Model of Psychotic Disorder." *Psychological Medicine* 39: 179–195. <https://doi.org/10.1017/S0033291708003814>.
- Verdoux, H., and J. van Os. 2002. "Psychotic Symptoms in Non-Clinical Populations and the Continuum of Psychosis." *Schizophrenia Research* 54: 59–65. [https://doi.org/10.1016/S0920-9964\(01\)00352-8](https://doi.org/10.1016/S0920-9964(01)00352-8).
- Wilson, T. W., D. C. Rojas, M. L. Reite, P. D. Teale, and S. J. Rogers. 2007. "Children and Adolescents With Autism Exhibit Reduced MEG Steady-State Gamma Responses." *Biological Psychiatry* 62: 192–197. <https://doi.org/10.1016/J.BIOPSYCH.2006.07.002>.

Supporting Information

Additional supporting information can be found online in the Supporting Information section.